

Wind Turbine Blade Fault Detection Using Wavelet Power Spectrum and Experimental Modal Analysis

Khalid F. Abdulraheem*[‡], Ghassan Al-Kindi *

* Faculty of Engineering, Sohar University, POB 44, PC-311, Sohar, Oman

(kaloodi2005@yahoo.com, gkindi@su.edu.om)

[‡]Corresponding Author; Khalid F. Abdulraheem, Postal address, POB 44, PC-311, Sohar, Oman, kaloodi2005@yahoo.com

Received: 13.09.2018 Accepted:16.11.2018

Abstract- The dynamic behaviour of modern multi-Megawatt wind turbines has become an important design consideration. The power generated by wind turbine depends mainly on the interaction between the rotating blades and flowing wind. The aerodynamics characteristics and structure integrity of the blade contribute significantly to the performance and availability of wind turbine machine. This paper demonstrates the application of wavelet transform and vibrational modal analysis to evaluate the dynamic characteristics and structure integrity of wind turbine blades. The wavelet power spectrum (WPS) has been calculated for different cracked-beam conditions and vibration sensors locations. The results reveal the effectiveness of the wavelet power spectrum over the traditional FFT spectrum to identify the existence of the crack in the wind turbine blade. Moreover, a mathematical model, which correlates the variation of the blade natural frequencies with the crack severity and location, is presented and validated with the experimental modal analysis data.

Keywords Vibration-Modal Analysis; Wind Turbine Blade Fault Detection; Wavelet Power Spectrum; Cracked Beam Model.

1. Introduction

The recent wind turbine machines driven base on the aerodynamic forces generated by the interaction between the winds and the blade airfoil. The integrity, stability and aerodynamic characteristics of the wind turbine blade structure plays a vital role in the power generation of the wind turbine system as the blades grow longer and more flexible in the modern wind turbine machines. Furthermore, the wind turbine blades experience various types of loading and severe working condition during the operation of wind turbine. The fatigue crack is the common defect experiences by the wind turbine blade which initiate due to the variable force applied by the wind while flowing with variable speed. The progression of the fatigue crack is fast as the blade subjected to extreme working conditions. To avoid the catastrophic failure and its fatal consequences and high cost replacement process, an effective continuous blade health monitoring and crack detection techniques are required to introduce.

Various fault diagnostics techniques using different measured variables : vibration [1], acoustic and noise emission [2], electrical current [3], generated power curve characteristics [4,5], etc. and signal processing: time domain, frequency domain and wavelet analyses are investigated to monitor the health condition of the wind turbine components

(blades, structure, gearbox, bearings, electrical generator, etc.) and develop a maintenance strategy [6], a state of art survey has given by Qiao and Lu [7]. The modal hammer and electrodynamic shaker tests are performed by Tartibu, L.K. et. al. [8] to identify the modal frequencies for the stepped beam in flap-wise, edge-wise and torsional orientation. To avoid the resonance, the main excitation force frequencies are identified to enable the blade designer to ensure that these are not close to the blade natural frequencies. Ulriksen, et.al. [9] discuss the application of the finite element modal analysis to evaluate the structural health condition of a small wind turbine blade. The modal analysis parameters have been validated with an experimental test. Griffith and Carne [10] studied the instrumentation layout, support conditions, excitation type of an experimental modal analysis of a nine-meter blade size carefully designed to reduce the test uncertainty in evaluating the modal parameters. An operational modal analysis has been performed by Lorenzo, et. al. [11], the experimental results show a decrease in the natural frequencies and an increase of the estimated modal damping of the faulty structure compared with a healthy one. Abdulraheem and Al-Kindi [12] investigate the influence of the wind turbine blade fault characteristics on the experimental modal analysis parameters (modal frequency, damping ratio, and modal shape) for blade fault diagnostics. In this study, the wind turbine blade is approximated as a

stepped beam and the results show the potential correlation between the modal parameters and blade fault conditions.

The structural dynamics of a bend-twist coupled full-scale section of an eight-meter wind turbine blade section cut from a 23-meter wind turbine blade hollow structure has been analyzed by Luczak, et.al. [13] using an experimental modal analysis to explore the effect of the structure support conditions on the correlation between the Finite Elements simulation and experimental shaker-modal analysis. The results clearly exhibit the influence of involving the blade support conditions on the accuracy of the simulated model. Two sets of sensors (i.e. strain gauges and accelerometers) are mounted in span-wise direction of a blade with surface defects subjected to fatigue tests in flap direction, Yang W et. al. [14]. The acquired signals analysed in time and frequency domains to monitor the surface crack propagation along the fibers of the composite material. Abdulraheem and Al Kindi [15] performed a finite element modal analysis to demonstrate the variation in the FRF modal frequencies with blade fault location and size. The FRF peaks (natural frequencies) for all vibrational modes are less, as the crack size is developed. However, the modal frequencies are higher when the fault location is close the free end of the WT blade.

In Coscetta et. al. [16], set of fiber-optic strain gauge and accelerometer sensors distributed along a WT composite blade of a 14 m long to monitor the blade deformation. The frequency spectrum of the dynamics strain at free end and the clamped end calculated, the spectrum first peak frequency (natural frequency) is less when more load applied to the blade; however, the strain magnitude is more at the free end compare to the clamped end. Zhang and Jackman [17] evaluate the application of image processing techniques for WT blade surface cracks detection. The image inspection shows promise as a maintenance approach for in-service wind turbine blades. The CWT with Gaussian wavelet applied by Ulriksen et. al. [9] to structural mode shape signals to assess the WT blade structural damage. A one-dimensional wavelet transform is performed to capture the irregularities in the blade modal shape signal, which introduced as consequences of the presence blade damage.

This paper, presents a novel application of Wavelet Transform as an effective signal processing technique for nonstationary signal to analyse the response of the stepped beam to harmonics excitation as an approach for crack detection in wind turbine blade. A mathematical model for an emulated blade (i.e. a cantilever stepped cracked beam) using energy approach has been developed and validated with experimental data. The model defines the correlation

between the beam natural frequencies and crack characteristics (i.e. size and location).

2. Modelling of Transverse Loaded Cantilever Cracked Beam

A rectangular section cantilever beam with surface crack subjected to harmonics force, $F(t) = F_o \sin \omega t$ is assumed in this model. The crack, which introduces a local flexibility, can be introduced as a massless rotational spring with stiffness, K_t , as shown in Figure 1. During one-half of the cycle, the vibration curvature is positive, the crack is fully closed and there is no discontinuity in flexural stiffness of the beam. In this case, the equivalents beam stiffness (K_c), which assumed as an intact beam, given as [18,19]:

$$K_c = \frac{1}{C_c} = \int_0^L EI [\Phi''(x)]^2 dx = \frac{\pi^4 EI}{32 L^3} \quad (1)$$

Where, C_c is the flexibility of intact beam, EI is the beam flexural rigidity and $\Phi(x)$ is the vibrational mode shape (curvature) of the beam. In the second half of the cycle, the curvature of the beam is negative and the crack is fully open with change in the local stiffness. In this situation, the total equivalent beam stiffness (K_o) is:

$$K_o = \frac{1}{C_o} = \frac{K_t K_c}{K_t + K_c} = \frac{K_c}{1 + \Delta C K_c} \quad (2)$$

Where, C_o is the total flexibility = $C_c + \Delta C$, ΔC is the additional flexibility in the beam due to existence of the crack and can be determined as:

$$\Delta C = \frac{1}{K_t} = \frac{18 L_c^2 \pi (1-\nu^2)}{E b h^2} f\left(\frac{a}{h}\right) \quad (3)$$

Where a is the crack depth, L_c is the crack location, b is width and h is the thickness of the beam and ν is poisson's ratio.

The correction function $f(a/h)$ is obtained from the following equation:

$$f\left(\frac{a}{h}\right) = 0.627 \left(\frac{a}{h}\right)^2 - 1.045 \left(\frac{a}{h}\right)^3 + 4.595 \left(\frac{a}{h}\right)^4 - 9.974 \left(\frac{a}{h}\right)^5 + 20.30 \left(\frac{a}{h}\right)^6 - 33.03 \left(\frac{a}{h}\right)^7 + 47.106 \left(\frac{a}{h}\right)^8 - 40.756 \left(\frac{a}{h}\right)^9 + 19.60 \left(\frac{a}{h}\right)^{10} \quad (4)$$

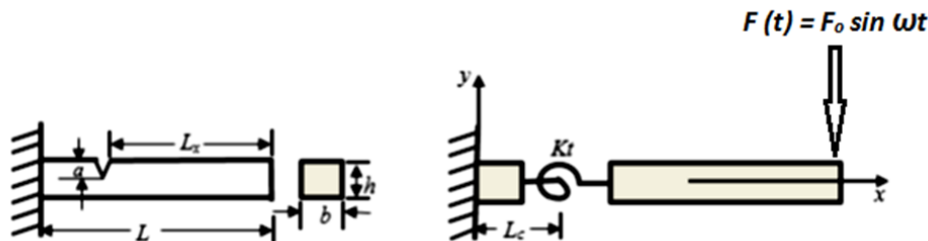


Fig. 1. Geometry of cantilever beam with crack modeled as torsional spring.

During the transverse vibration of the cracked beam, the time variant beam stiffness is oscillating between K_o and K_c , and can be modelled as a simple periodic function of, [20]:

$$K(t) = K_o + \frac{K_c - K_o}{2} [1 + \cos(\omega t)] \tag{5}$$

Where, ω is the excitation force frequency. At $\omega = 2 n \pi$, ($n=1,2,3\dots$), the crack is fully closed and $K(t) = k_c$ and with $\omega = (2n-1) \pi$, ($n=1,2,3\dots$), the crack is fully-open and $K(t) = K_o$. The beam equation of motion for harmonic excitation is:

$$M\ddot{y} + C\dot{y} + K(t) y = F_o \sin \omega t \tag{6}$$

The above cracked beam model has been developed and solved in MATLAB/Simulink environments. Figure 2 shows the transverse displacement response $y(t)$, solution of Equation 6, for healthy and cracked beam (with specifications shown in experimental setup section), the response non-linearity is clear in cracked beam signal as a result of time varying stiffness $K(t)$.

As illustrated in Figure 2, the time variant cracked beam stiffness. $K(t)$ generates a non-stationary vibrational response, $y(t)$ with frequency content varying with time. The normal FFT spectrum analysis is efficient only while dealing with stationary signal, in this paper the application of wavelet transform spectrum as a non-stationary signal analysis tool is investigated for crack detection in a cantilever beam. The variation of the modal natural frequencies as a result of the variation in crack stiffness based on the Rayleigh's quotient for healthy and cracked beams is expressed as [21,22]:

$$\frac{\Delta\omega_n}{\omega_n} \cong \frac{\left(\frac{M_n^2}{2K_t}\right)}{2U_n} \tag{7}$$

Where $\Delta\omega_n$ is the difference between the n^{th} modal natural frequency of healthy and cracked beam and M_n is the developed resisting modal bending moment at crack location in n^{th} mode and given by:

$$M_n = E_n I [\phi_n''(\beta)]^2 \tag{8}$$

E_n is the modal corrected young modulus of the beam in n^{th} mode, I is the moment of inertial of beam section, $\phi_n''(\beta)$ is the curvature of the n^{th} mode shape of the un-cracked beam, β is the normalized crack location = L_c/L . U_n is the total modal strain energy stored in the un-cracked beam in the n^{th} mode and defined by, [21]:

$$U_n = \frac{L}{2} \int_0^1 EI [\phi_n''(\beta)]^2 d\beta \tag{9}$$

Substituting equations 5 and 6 in equation 4, we got:

$$\frac{\Delta\omega_n}{\omega_n} \cong \frac{EI [\phi_n''(\beta)]^2}{2K_t L \int_0^1 [\phi_n''(\beta)]^2 d\beta} \tag{10}$$

or

$$\frac{\Delta\omega_n}{\omega_n} \cong \Psi_n \frac{[\phi_n''(\beta)]^2}{K_t} \tag{11}$$

where Ψ_n is the crack independent variable and expressed as:

$$\Psi_n = \frac{EI}{2L \int_0^1 [\phi_n''(\beta)]^2 d\beta} \tag{12}$$

For three-stepped beam shown in Figure 2, the total modal strain energy written as:

$$U_n = \frac{L}{2} \left[\int_0^{L_1/L} EI_1 [\phi_n''(\beta)]^2 d\beta + \int_{L_1/L}^{(L_1+L_2)/L} EI_2 [\phi_n''(\beta)]^2 d\beta + \int_{(L_1+L_2)/L}^1 EI_3 [\phi_n''(\beta)]^2 d\beta \right] \tag{13}$$

In matrix form using three modal natural frequencies, Equation 10 is expressed as:

$$\begin{Bmatrix} \frac{\Delta\omega_1}{\omega_1} \\ \frac{\Delta\omega_2}{\omega_2} \\ \frac{\Delta\omega_3}{\omega_3} \end{Bmatrix} = \begin{bmatrix} \Psi_1 & 0 & 0 \\ 0 & \Psi_2 & 0 \\ 0 & 0 & \Psi_3 \end{bmatrix} \begin{bmatrix} [\phi_1''(\beta)]^2 \\ [\phi_2''(\beta)]^2 \\ [\phi_3''(\beta)]^2 \end{bmatrix} \begin{Bmatrix} \frac{1}{K_t} \\ \frac{1}{K_t} \\ \frac{1}{K_t} \end{Bmatrix} \tag{14}$$

Knowing three natural frequencies of healthy and cracked beam, Equation 14 can be plotted with normalized crack location β varies from 0 to 1. The intersection point of the three curves will specify the crack spring stiffness (K_t) and the location β . Furthermore, the obtained value of the K_t is used to determine the crack depth (a) using Equation (3). A MATLAB code is developed to graph the solution of Equation (14). The model has been validated by a stepped beam of $L_1=125$ mm, $L_2=150$ mm, $L_3=150$ mm and $W_1=50$ mm, $W_2=40$ mm, $W_3=30$ mm (Figure 3) using the

experimental modal analysis results published by same authors in [6]. The experimental modal analysis (impact hammer test) Frequency Response Function (FRF) for healthy and beam with crack depth of $a=4$ mm and crack location $L_c=200$ mm, measured form the free end are shown in Figure 4. First three modal frequencies (peaks) in the FRF have been selected to run the model.

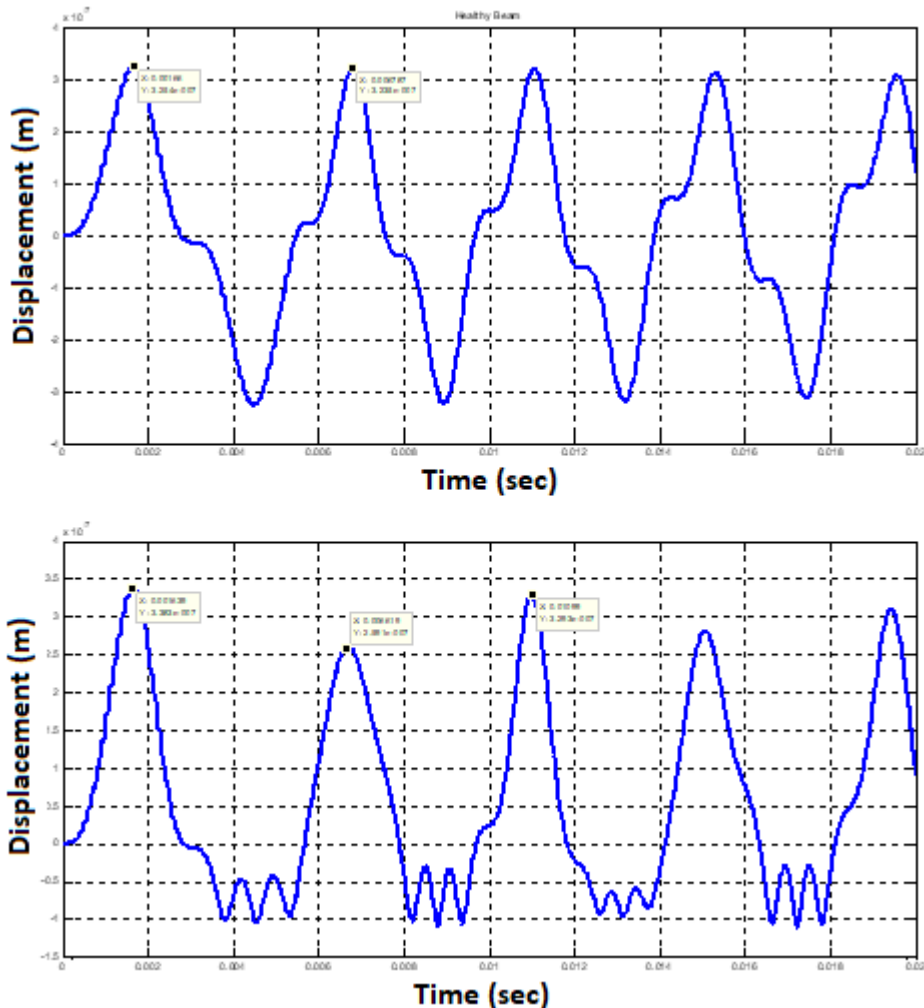


Fig. 2. The modelled Transverse Displacement $y(t)$ -Equation 6- of (a) Healthy Beam and (b) Cracked beam.

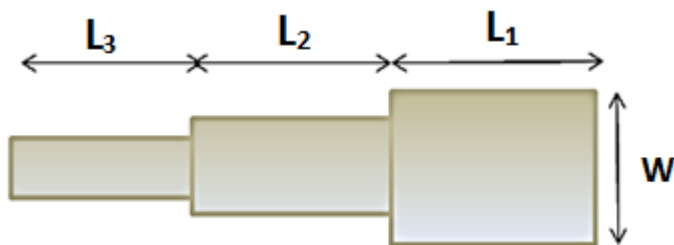


Fig. 3. Three-stepped beam used in this study.

Figure (5) shows the variation of crack stiffness (K_f) with normalized crack location ($\beta=L_c/L=0.470$), for the first three

modal frequencies. The intersection point of the three curves is at $\beta= 0.445$ with $K_f= 8.962$ N/m. The location of the crack

has been identified with relative error of 5%. Furthermore, the crack depth can be evaluated using Equation 3.

3. Wavelet Transform

The wavelet transform is the inner product of a time domain signal $x(t)$ with the translated and dilated wavelet-base function $\psi(t)$, [23]:

$$W(a, b) = \langle x(t), \psi(t) \rangle = \int x(t) \psi(t)_{a,b}^* \quad (15)$$

Where the scaling parameter, a , acts to vary the time scale of the wavelet function and dilation parameter, acts to translate the wavelet function across the signal $x(t)$.

The impulse-response wavelet is selected in this paper to represent the wavelet-based function, as it is with more similarity to the cracked beam response characteristics that enhance the amplitude of the generated wavelet transform coefficients. The impulse-response wavelet defined as, [24]:

$$\psi(t) = A e^{-\frac{\beta}{\sqrt{1-\beta^2}} \omega_c t} \sin(\omega_c t) \quad (16)$$

Where β is the damping factor and ω_c is the wavelet centre frequency, and A is an arbitrary scaling factor. Figure 6 shows the impulse wavelet and its power spectrum.

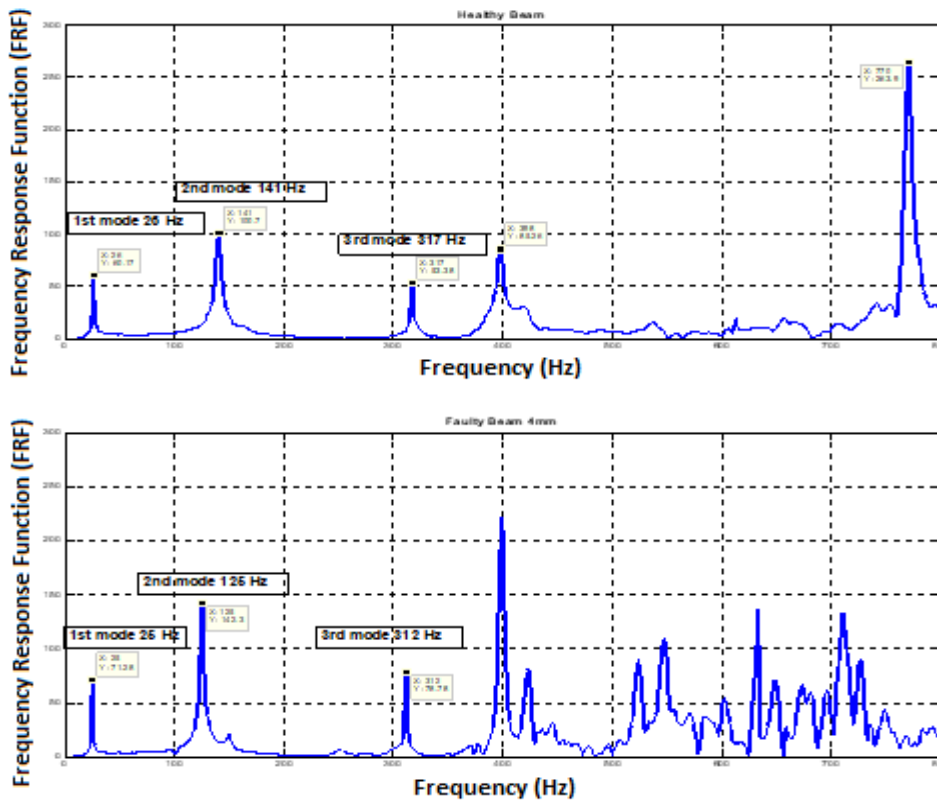


Fig. 4. The FRF of hammer test response for (a) healthy beam (b) cracked beam

To extract the frequency content of wavelet transform coefficients, the scale Wavelet Power Spectrum (WPS) is computed as, [24]:

$$WPS(a, \omega) = \int_{-\infty}^{\infty} |SEWT(a, \omega)|^2 d\omega \quad (17)$$

Where, $SEWT(a, \omega)$ is the Fourier Transform of $W(a, b)$.

4. Experimental Setup

An Experimental Model testing with Shaker excitation has been performed for the beam with different health

conditions. Figure 7 shows the experimental setup. A sinusoidal and random excitation forces applied to the cantilever-stepped beam (Figure 3) via a B&K Modal Exciter type 4824 with power amplifier type 2732. The exciter connected to the output port of the B & K DAQ module type 3160-A-042. Three B&K ICP accelerometers type 4507B connected to the input ports of the data acquisition module to measure the acceleration response of the cantilever beam at three different locations along the beam length. A Force Transducer type 8230 used to acquire the applied excitation signal to the beam. A Pulse10 (B&K software) software has been used to record and analyse the acquired signals.

5. Time Domain Analysis

The time domain signals of the excitation harmonics force at frequency of 300 Hz and the corresponding responses (acceleration signals) at the free-end of the healthy and cracked beam are shown in Figure 8. A significant increase in the acceleration amplitude of the faulty beam compared with the healthy one can be recognized, i.e. the Peak to-Peak amplitude for faulty is 102.7 m/s² and 47.4 m/s² for healthy beam. This is due to the decrease of the beam stiffness because of introducing a crack in the beam structure. To study the change in the vibration amplitude along the beam length, Figure 9 shows the variation of the vibration magnitudes of a healthy beam in three different locations. Location 1 (at the free end of the beam -near the excitation point), location 2 at the mid length of the beam, and location

3 near the clamp end of the cantilever beam. As expected, the vibration amplitude is less as the measuring point moves toward the clamp end. This is also to validate the vibration measuring process.

The same variation for cracked beam is shown in Figure 10. The vibration amplitude is more at location 2 (near the crack position) compare to free and clamp ends. However, the vibration at free-end is still more than at the clamp-end. The beam local stiffness is dropped at crack location that leads develop the vibration amplitude. The non-uniformly of vibrational magnitude along its length (compare with the healthy beam) is a good indication of crack presence.

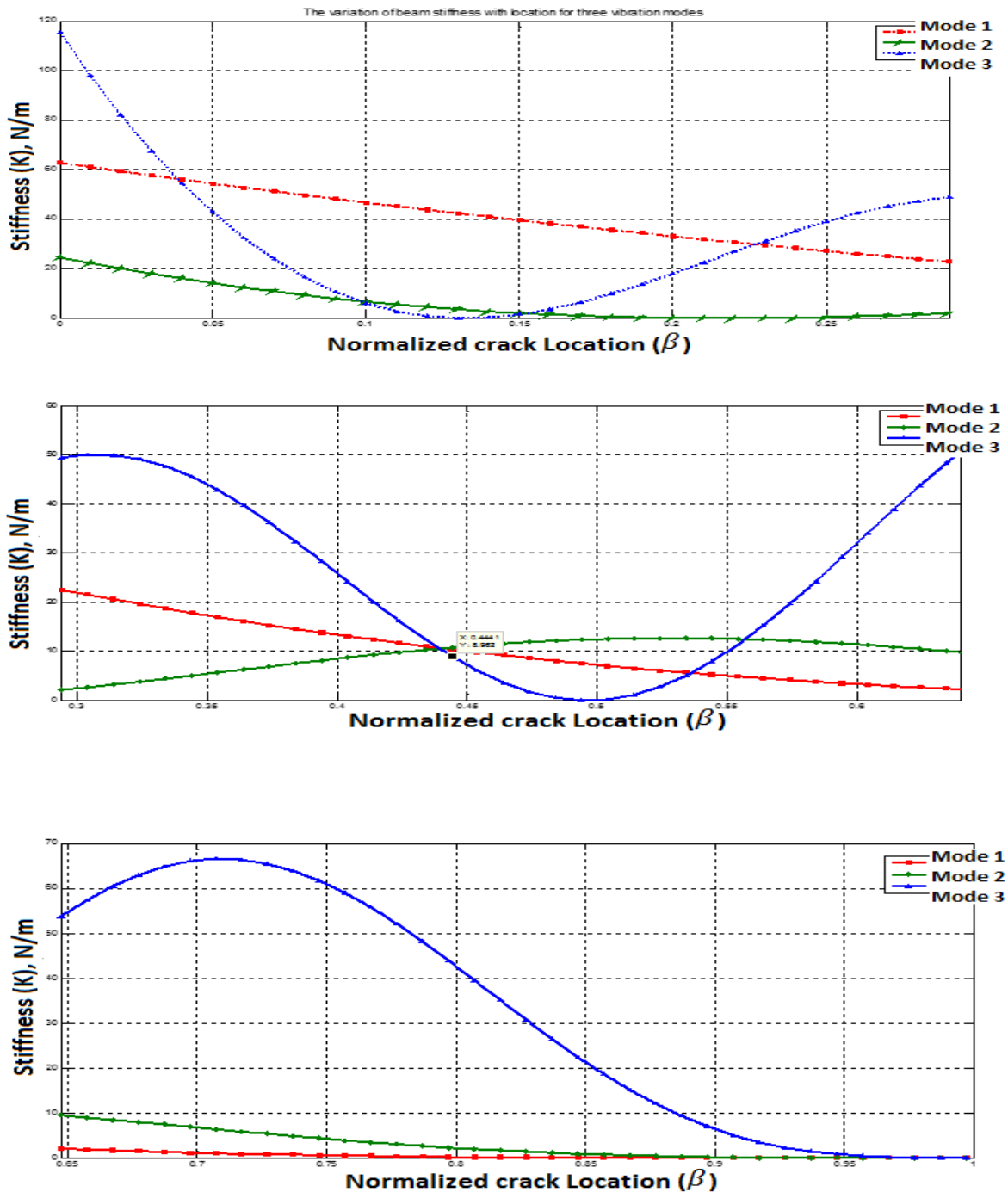


Fig. 5. The variation of the three steps beam stiffness with the normalized location for three vibration modes.

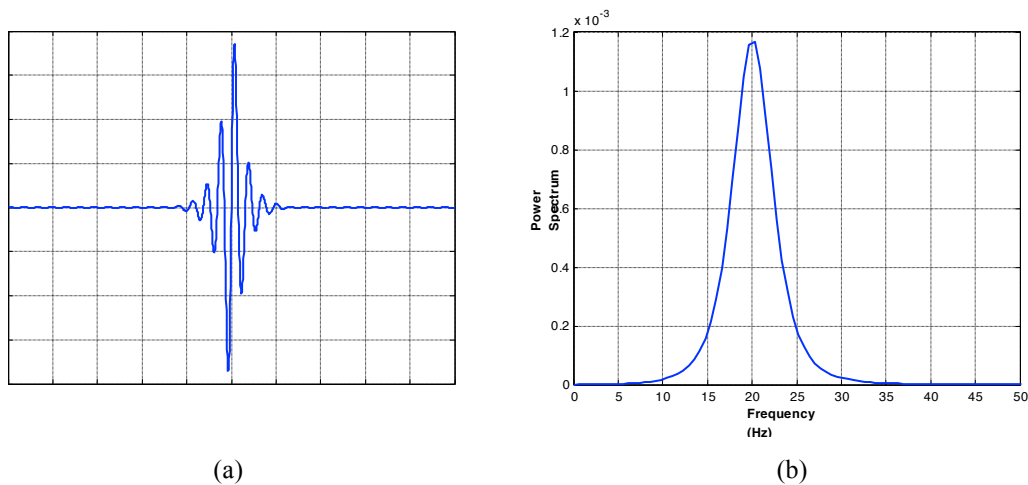


Figure 6. (a) The impulse wavelet time waveform, (b) Its FFT-spectrum.

6. Frequency Domain Analysis- FFT Power Spectrum

Figure 11 depicts the variation of the FFT spectrum of the applied force with excitation frequency of 300 Hz and beam vibrational response (i.e. acceleration signal) at the different locations along the beam length. The spectrum shows peaks at the force excitation frequency and its harmonics, however, there is no clear-recognized change in the spectrum amplitude and/or the frequency contents (peaks) with the sensor locations can be detected.

7. Time-Frequency Analysis- Wavelet Power Spectrum (WPS)

To tackle the drawbacks of the FFT-spectrum while dealing with non-stationary signals, the wavelet analysis has been performed for the beam vibrational signals. The Wavelet Power Spectrums (WPS) of the applied force and vibrational signals have been calculated through a MATLAB code based on Equation 5.

Figure 13 shows the WPS of the excitation force and the vibrational response of the healthy beam at the three-accelerometer locations. The variation of the WPS along the

beam length is relatively easier to recognize compare with the FFT-spectrum. The difference in the overall level of the WPS for the healthy and cracked beams can be clearly detected in Figure 14, for the three response measuring positions, compared to the same using the FFT spectrum that shown in the previous section. This prove the effectiveness of the wavelet transform in dealing with nonstationary signals over the FFT-spectrum and can be applied as promising technique for beam fault diagnostics. Moreover, the variation in the WPS for healthy and cracked beam is more in position 2 when the sensor is more close to the crack location as shown in Figure 14b; this is due to that the beam stiffness drop in this region.

Figure 12, shows the FFT spectrum of the acceleration response at location 1 for the healthy and faulty beams. There is no detectable variation in the FFT spectrum magnitude and/or frequency contents (peaks) can be recognized and it is much difficult to detect the presence of the crack by monitoring the FFT spectrum. The reason behind that the vibration signal for the healthy beam is non-stationary as a result of the nonlinear variations in the cracked beam stiffness during the close-open cycles of beam bending oscillations.

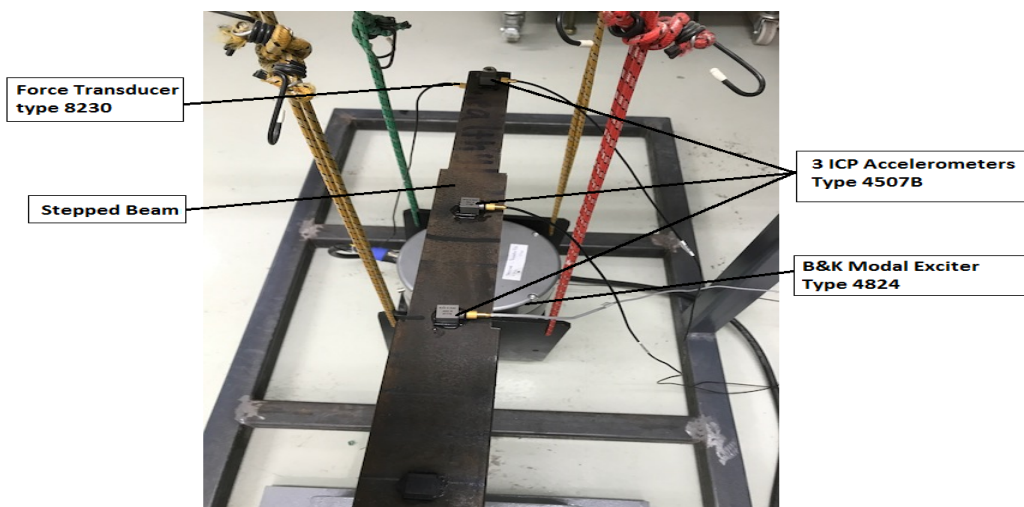
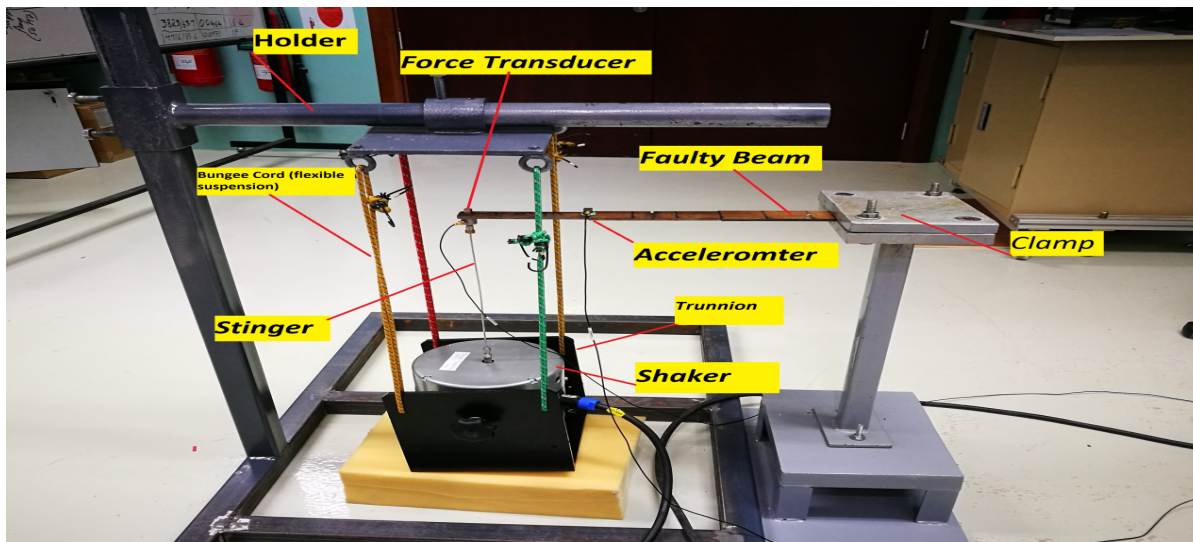


Fig.7. Shaker-Excitation experimental setup.

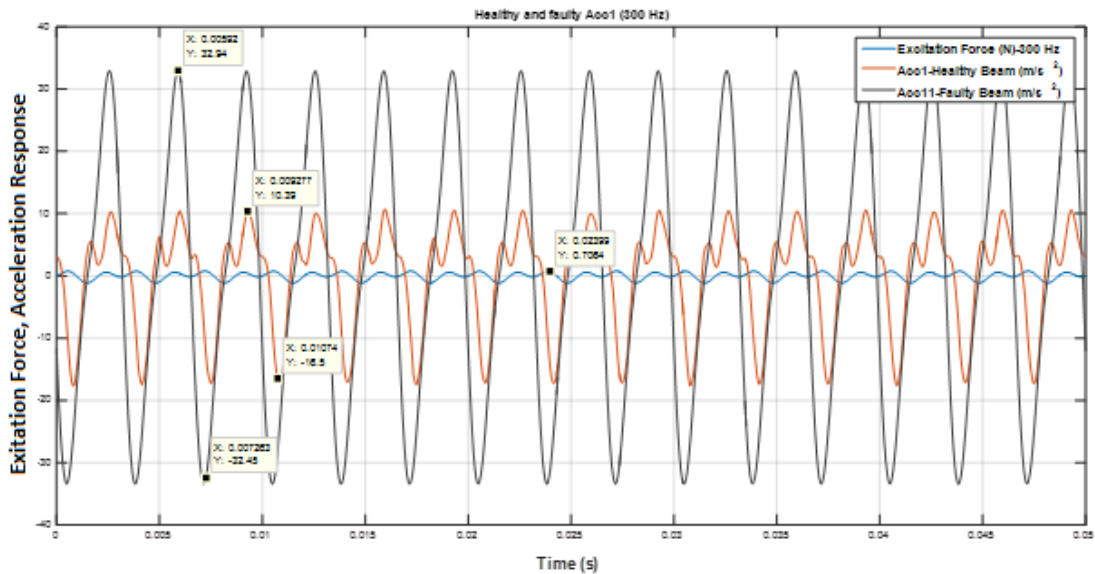


Fig. 8. Time domain signals of the excitation force the acceleration response for the healthy and cracked beams.

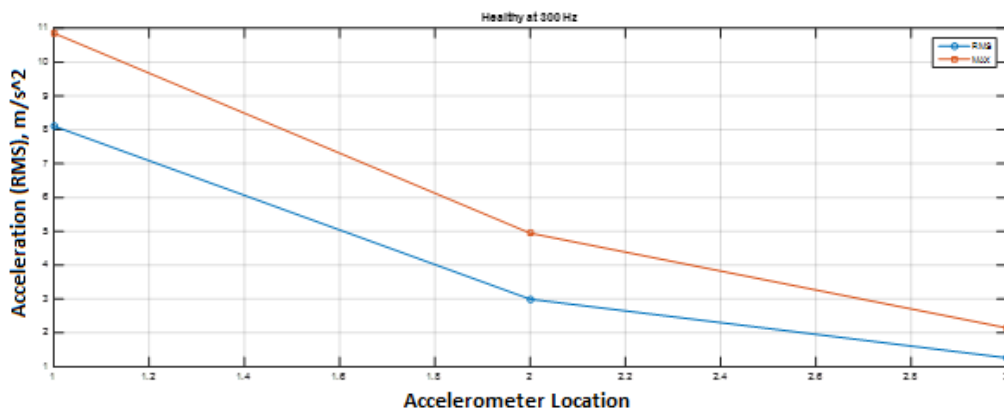


Fig. 9. The variation in the vibration amplitudes at different measuring locations for healthy beam.

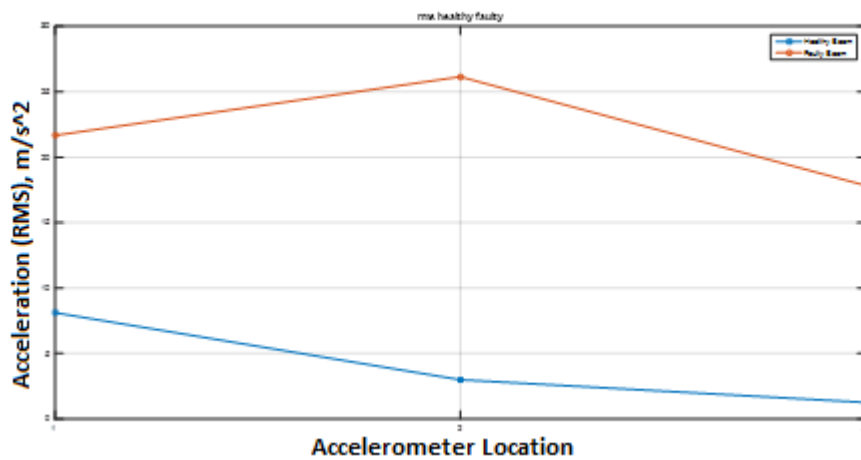


Fig. 10. The variation in the vibration amplitudes at different measuring locations for cracked beam.

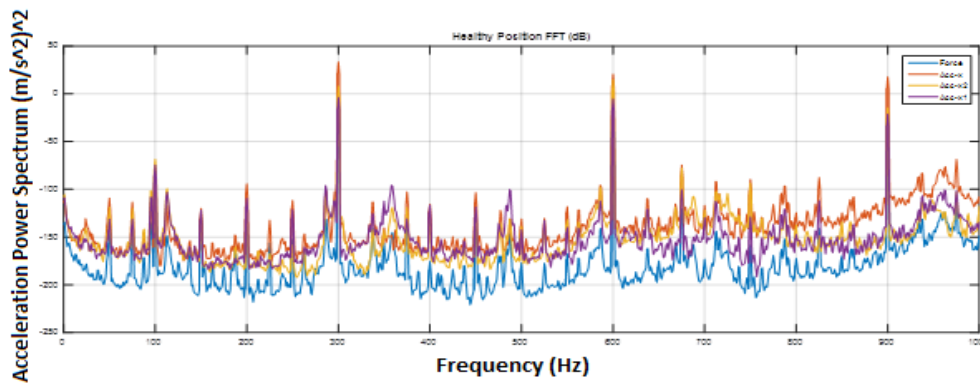


Fig. 11. the FFT power spectrums of the excitation force and beam response at three different locations.

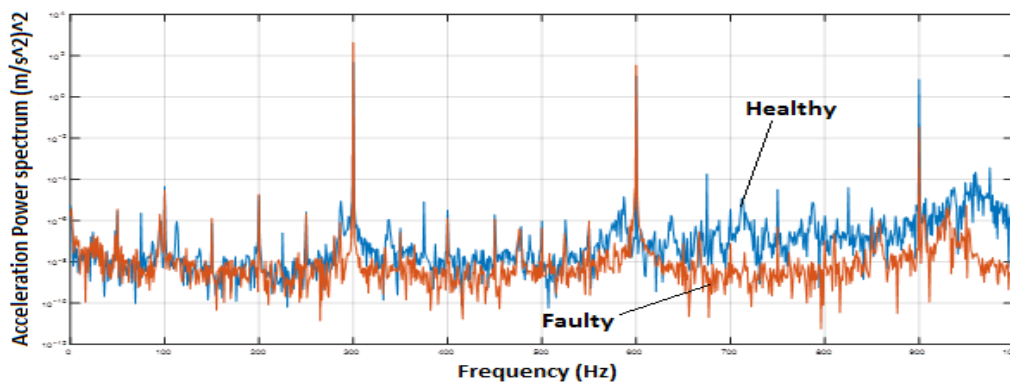


Fig. 12. The FFT spectrums of location 1 accelerometer of healthy and cracked beams.

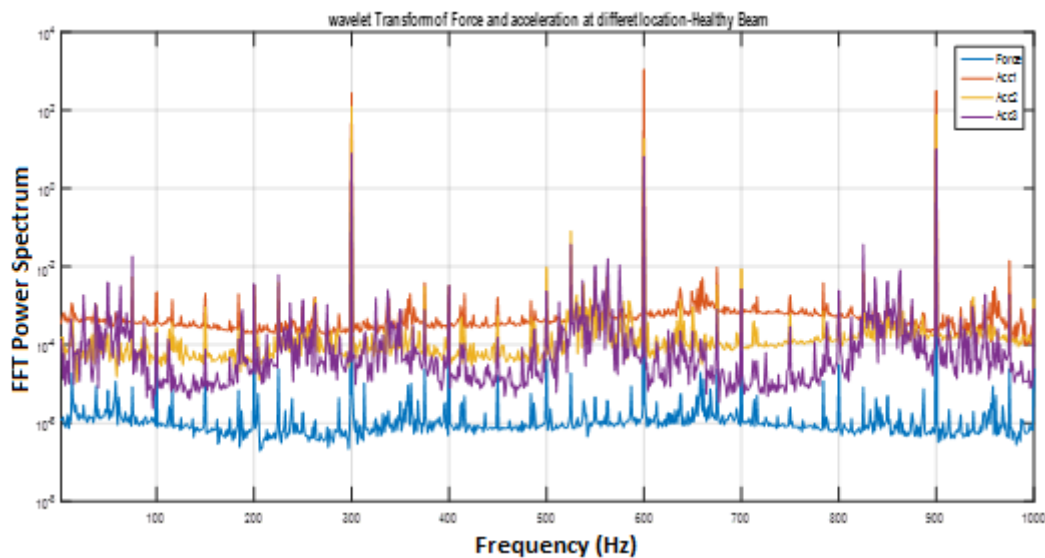


Fig. 13. The WPS of the excitation force and beam response at three different locations.

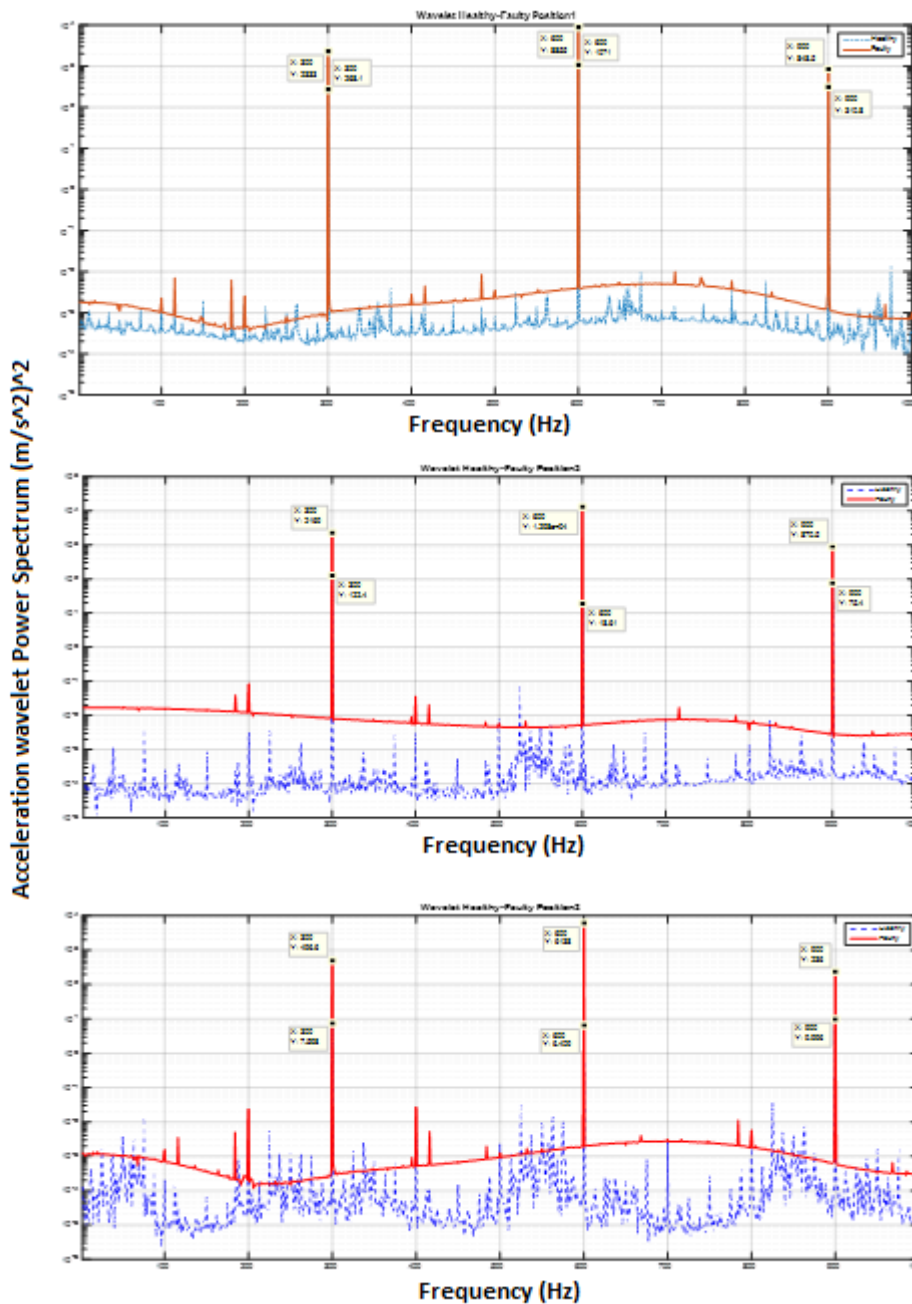


Fig. 14. The WPS of the beam vibrational response for healthy and cracked beams at: (a) Location 1; (b) Location 2 and (c) Location 3.

8. Conclusions

The cracked wind turbine blade generates a non-stationary signal when the wind dynamic force excites it during the operation of wind turbine machine. This paper investigates the application of wavelet transform as a multi-resolution technique to process of non-stationary signals for wind turbine blade fault detection. The results show the effectiveness of the WPS to distinguish between the healthy and cracked stepped beam, which is used to approximate the wind turbine blade over the normal FFT spectrum. The

variation of the overall WPS amplitudes is more at the location which is more close to the crack, which can be applied as indication to locate the position of the defect along the blade. The peak frequencies and its harmonics are identical to the excited force frequency for both the healthy and faulty blade and at all the locations throughout the blade. Furthermore, a model describes the relationship between the beam stiffness/crack size and the change in the blade natural (modal) frequencies is presented and validated using experimental data acquired using impact hammer modal test. The model can be used based on the

experimental data obtained from healthy blade and the change in the modal frequencies (peaks at FRF) during the operation of wind turbine as indicator to detect the presence of the crack and estimate its size.

Acknowledgements

This is to acknowledge that this paper is a part of research project entitled “Automatic condition Monitoring and predictive diagnostics as applied to Wind Turbines” no. ORG/SU/14/010 funded by “The Research Council” (TRC) /Oman.

References

- [1] D. Koulocheris, G. Gyparakis, A. Stathis, T. Costopoulos (2013), *Vibration Signals and Condition Monitoring for Wind Turbines*, Engineering, vol.5, pp. 948-955.
- [2] J. Van Dam, Leonard J. Bond (2015), *Acoustic emission monitoring of wind turbine blades*, SPIE 9439, *Smart Materials and Non-destructive Evaluation for Energy Systems*, 94390C; doi:10.1117/12.2084527.
- [3] Pizzo, A & Di Noia, L.P. & Lauria, D & Rizzo, R & Pisani, Cosimo. (2015); *Stator current signature analysis for fault diagnosis in permanent magnet synchronous wind generators*; 2015 IEEE International Conference on Renewable Energy Research and Applications (ICRERA); DOI: 10.1109/ICRERA.2015.7418470
- [4] M. Carmona, M. A. Sanz-Bobi (2016), *Normal power generation area of wind turbines for the detection of abnormal performance*, 2016 IEEE International Conference on , *Renewable Energy Research and Applications (ICRERA)*, pp. 335-340.
- [5] Rodrigo J. de Andrade Vieira ; Miguel A. Sanz-Bobi (2015), *Power curve modelling of a wind turbine for monitoring its behaviour*, 2015 IEEE International Conference on Renewable Energy Research and Applications(ICRERA),DOI:10.1109/ICRERA.2015.7418571
- [6] Z. Hajej ; N. Rezg ; M. Bouzoubaa (2017); *An integrated maintenance strategy for a power generation system under failure rate variation (case of wind turbine)*; 2017 IEEE International Conference on Renewable Energy Research and Applications (ICRERA);DOI: 10.1109/ICRERA.2017.8191175.
- [7] W. Qiao, D. Lu (2015), *A Survey on Wind Turbine Condition Monitoring and Fault Diagnosis–Part II: Signals and Signal Processing Methods*, IEEE Transactions on Industrial Electronics, vol.62 (10), pp. 6546 – 6557.
- [8] Tartibu, L.K., Kilfoil, M. and Van Der Merwe, A.J. (2012), *Modal Testing Of A Simplified Wind Turbine Blade*, *International Journal of Advances in Engineering & Technology*, vol. 4(1), pp.649-660.
- [9] M. D. Ulriksen, J. F. Skov, K. A. Dickow, P. H. Kirkegaard and L. Damkilde (2013) , *Modal Analysis for Crack Detection in Small Wind Turbine Blades*, *Key Engineering Materials*, vol. 569-570, pp. 603-610.
- [10] D. Todd Griffith Thomas G. Carne (2010), *Experimental Modal Analysis of 9-meter Research-sized Wind Turbine Blades*, *Proceedings of the IMAC-XXVIII February 1–4, Jacksonville, Florida USA Society for Experimental Mechanics Inc.*
- [11] E. D. Lorenzo, G. Petrone, S. Manzato, B. Peeters, W. Desmet and F. Marulo (2016), *Damage detection in wind turbine blades by using operational modal analysis*, *Structural Health Monitoring*, vol. 15(3), pp. 289-301.
- [12] Khalid F. Abdulraheem, Ghassan Al-Kindi (2017), *A Simplified Wind Turbine Blade Crack Identification Using Experimental Modal Analysis (EMA)*, *International Journal of Renewable Energy Research*, vol.7 (2), pp. 715-722.
- [13] M. Luczak, S. Manzato, B. Peeters, K. Branner, P. Berring, and M. Kahsin (2014), *Updating Finite Element Model of a Wind Turbine Blade Section Using Experimental Modal Analysis Results*, *Shock and Vibration*, Article ID 684786, 12 pages, 2014. doi:10.1155/2014/684786.
- [14] Yang W, Lang Z, Tian W. (2015), *Condition Monitoring and Damage Location of Wind Turbine Blades by Frequency Response Transmissibility Analysis*, *IEEE Transactions on Industrial Electronics*, vol. 62(10), pp. 6558-6564.
- [15] Khalid F. Abdulraheem, Ghassan Al-Kindi (2015), *Wind Turbine Blade Fault Detection Using Finite Element-Modal Analysis*, *International Journal of Applied Engineering Research*, vol. 10(21), pp. 42287-42292.
- [16] A. Coscetta, A. Minardo, Lucio Olivares (2017), *Wind Turbine Blade Monitoring with Brillouin-Based Fiber-Optic Sensors*, *Journal of Sensors*, Article ID 9175342, 5 pages, doi:10.1155/2017/9175342.
- [17] H. Zhang and J. K. Jackman (2014), *Feasibility of Automatic Detection of Surface Cracks in Wind Turbine Blades*, *Wind Engineering*, vol. 38(6), pp. 575–586.
- [18] S.M. Cheng, X.J. Wu, W. Wallace and A.S.J. Swamidias (1999), *Vibrational response of a beam with a breathing crack*, *Journal of Sound and Vibration*, vol. 225(1), pp.201–208.
- [19] M. Rezaee, R. Hassannejad (2010), *Free Vibration Analysis of Simply Supported Beam with Breathing Crack Using Perturbation Method*, *Acta Mechanica Solida Sinica*, vol. 23: pp. 459-470.
- [20] M. Rezaee and R. Hassannejad (2010), *Damped free vibration analysis of a beam with a fatigue crack using energy balance method*, *International Journal of Physical Sciences*, vol. 5(6), pp. 793–803.
- [21] D.P. Patil and Sukhendu Maiti (2003), *Detection of multiple cracks using frequency measurements*, *Engineering Fracture Mechanics*, vol. 70(12), pp.1553-1572.

- [22] W.M. Ostachowicz, M. Krawczuk (1991), Analysis Of The Effect Of Cracks On The Natural Frequencies Of A Cantilever Beam, *Journal of Sound and Vibration*, vol. 150(2), pp.191-201.
- [23] Mallat, S. (1999): a wavelet tour of signal processing, 2nd edition, Academic Press.
- [24] Al-Raheem, Khalid F., Roy, A., Ramachandran, K. P., Harrison, D.K. and Grainger, S. (2008), Application of Laplace Wavelet Combined with Artificial Neural Networks for Rolling Element Bearing Fault Diagnosis, *ASME J. of vibration and Acoustics*, 130 (5): 051007(1)-051007(9).